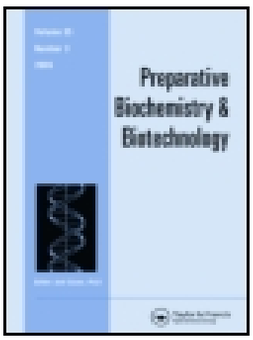

Preparative Biochemistry and Biotechnology

ISSN: 1082-6068 (Print) 1532-2297 (Online) Journal homepage: http://www.tandfonline.com/loi/lpbb20

Metabolic engineering of *Escherichia coli* W3110 strain by incorporating genome-level modifications and synthetic plasmid modules to enhance L-Dopa production from glycerol

Arunangshu Das, Neetu Tyagi, Anita Verma, Sarfaraz Akhtar & Krishna J. Mukherjee

To cite this article: Arunangshu Das, Neetu Tyagi, Anita Verma, Sarfaraz Akhtar & Krishna J. Mukherjee (2018): Metabolic engineering of *Escherichia coli* W3110 strain by incorporating genome-level modifications and synthetic plasmid modules to enhance L-Dopa production from glycerol, Preparative Biochemistry and Biotechnology, DOI: 10.1080/10826068.2018.1487851

To link to this article: https://doi.org/10.1080/10826068.2018.1487851

PREPARATIVE BIOCHEMISTRY AND BIOTECHNOLOGY
https://doi.org/10.1080/10826068.2018.1487851

Metabolic engineering of *Escherichia coli* W3110 strain by incorporating genome-level modifications and synthetic plasmid modules to enhance L-Dopa production from glycerol

Arunangshu Das[a], Neetu Tyagi[a], Anita Verma[a], Sarfaraz Akhtar[a], and Krishna J. Mukherjee[b]

[a]School of Biotechnology, Jawaharlal Nehru University, New Delhi, India; [b]Nagarjuna Fertilizers and Chemicals Limited, Kakinada, Andhra Pradesh, India

ABSTRACT

L-Tyrosine which is one of the terminal metabolites of highly regulated aromatic amino-acid biosynthesis pathway in *Escherichia coli* is a precursor for synthesis of L-Dopa. In this study, we report over production of L-Dopa by enhancing expression of rate limiting isoenzyme of shikimate kinase (aroL), chorismate synthase (aroC), aromatic-amino-acid aminotransferase (tyrB) and 3-phosphoshikimate 1-carboxyvinyltransferase (aroA) form a plasmid module harboring five enzymes under two inducible promoters converting shikimate to tyrosine. 4-hydroxyphenylacetate-3-hydrolase (hpaBC) which converts L-Tyrosine to L-Dopa was expressed constitutively from a separate plasmid module. Feedback deregulated expression of 3-Deoxy-D-arabinoheptulosonate-7-phosphate (DAHP) synthase (aroG*) replacing wild type aroG under its natural promoter led to enhancement of L-Dopa production. Deletion of transcriptional repressor tyrR and links to other competing pathways improved titers of L-Dopa. We focused on having a balanced flux by constitutive expression of pathway enzymes from plasmid constructs rather than achieving higher amounts of catalytic protein by induction. We observed glycerol when used as a carbon source for the final strain led to low acid production. The best performing strain led to decoupling of acid production and product formation in bioreactor. Fed batch analysis of the final strain led to 12.5 g/L of L-Dopa produced in bioreactor.

KEYWORDS

Genome; L-Dopa; metabolic engineering; pathway; plasmid modules

Introduction

Fifty years after the introduction of L-Dopa by George Cotzias as the successful proven treatment of Parkinson's disease and dopamine-responsive dystonia it still remains the only stand-alone drug available in the market.[1] The current L-Dopa industry turnover is around 250 tons per year with a market value of 101 million per year.[2] The bulk of L-Dopa produced by different industries worldwide comes from catalytic asymmetric hydrogenation of cinnamic acid which employs $[Rh(R,R)–DiPAMP)COD]^{+}BF4^{-}$ catalyst and is known as Monsanto process. The major drawbacks of the process are poor yield and lack of enantioselectivity.[3] Nevertheless, catalytic asymmetric synthesis of L-Dopa is going to be backbone of industry for quite a while from now as the alternatives will take time to emerge as viable industrial technologies in future. Pathway engineering and simultaneous bio-process optimization which has proven to be highly successful for many other commercial metabolites such as tyrosine, phenylalanine, tryptophan, and shikimic acid is a viable alternative which can replace the tedious chemical synthesis of L-Dopa in future.

Despite the fact that high titers of amino acid and shikimate have been obtained by pathway engineering the production of L-Dopa had only partial success. The putative reason which is most commonly overlooked is the energy intensive character of the aromatic amino-acid biosynthesis pathway (Fig. 1).[4–6] Metabolic engineering strategies for over production of metabolites have largely focused on directing major carbon fluxes toward desired product formation. Primarily these have been achieved either by removing fluxes from competitive pathways and over expression of pathway enzymes or by combinations of the two.[7–8] Over expression of pathway enzymes are normally achieved when respective genes cloned under a strong inducible promoter are harbored in plasmid modules. However, since the global circuitry of the cell is highly complex and all processes are ultimately interwined, over expression of pathway enzymes is only half way to the real solution. A major diversion of carbon flux leads to perturbations in the overall steady state of the cell. These perturbations propagate through the cell's metabolic and regulatory networks which lead to a diverse range of interdependent, transient responses in the abundance of metabolites, transcripts, and proteins.[9] Over expression of pathway enzymes for metabolite over production have two major disadvantages: (i) molecular resources have to be allocated for synthesis of higher amount of

CONTACT Arunangshu Das arujnu88@gmail.com School of Biotechnology, Jawaharlal Nehru University, New Delhi 110067, India.
Color versions of one or more of the figures in the article can be found online at www.tandfonline.com/lpbb.
Supplemental data for this article can be accessed online at http://dx.doi.org/10.1080/10826068.2018.1487851.

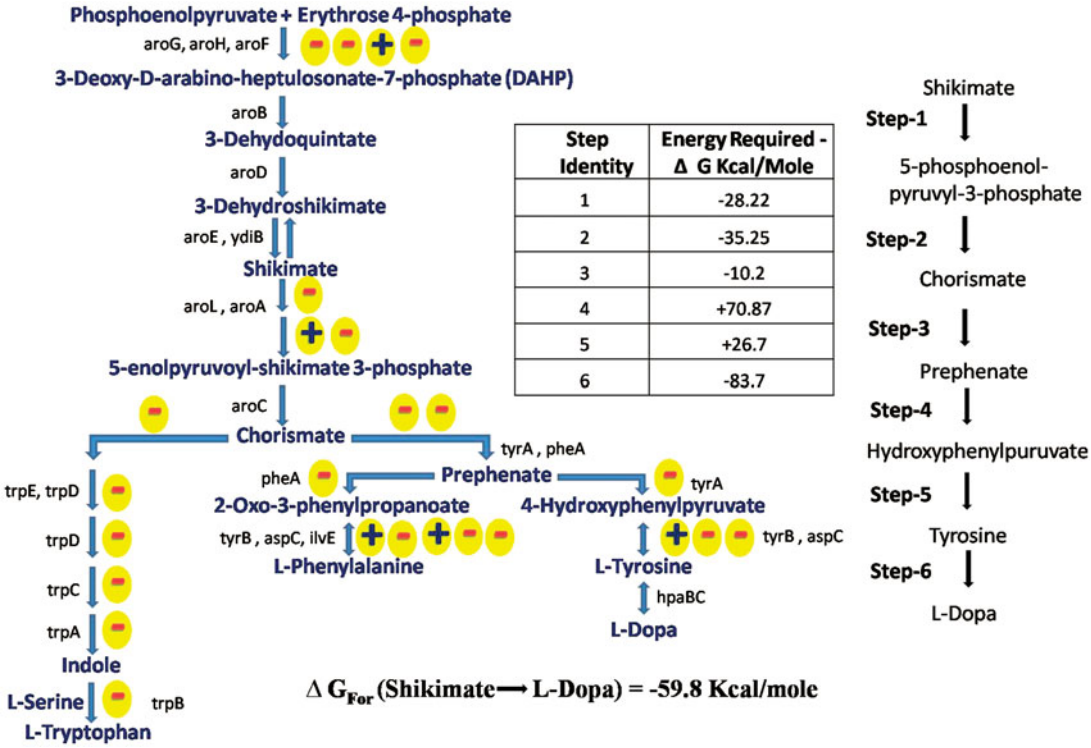

Step Identity	Energy Required - Δ G Kcal/Mole
1	-28.22
2	-35.25
3	-10.2
4	+70.87
5	+26.7
6	-83.7

Figure 1. Pathway for aromatic amino biosynthesis in *Escherichia coli.* Since the pathway is involved in synthesizing aromatic compounds from open chain highly oxidized substrates like glucose it is highly energy intensive. Energy requirement for conversion of Shikimate to L-Dopa has been provided for reference. The negative signs signify feedback/repression and positive signs signify induction.

protein and (ii) major carbon flux directed toward target metabolite synthesis leads to perturbations in steady-state metabolite pool of cell. When observed closely over expression of pathway enzymes partially antagonize diversion of major metabolic fluxes toward target metabolite synthesis and vice versa since molecular resources need to be allocated for protein synthesis also. The following can be demonstrated by a qualitative treatment provided in the book *Physical Biology of the Cell* by Philips, Rob et al. where multiplying the energetic cost of making each amino acid by its relative abundance in cell, it has been estimated that the average energetic cost to synthesize an amino acid is roughly 1.2 ATP equivalent (under aerobic condition in *Escherichia coli*) while incorporation of each amino acid to the growing polypeptide chain roughly require 4 ATP equivalent which include cost of attaching amino acid to t-RNA, and to power the movement of ribosome. Addition of a single amino acid to a growing polypeptide chain requires total 5.2 equivalent of ATP energy. Thus, it is clear that over expression of pathway enzymes has its own hidden cost which we often tend to ignore.[10] Furthermore, since active protein degradation is not a regular phenomenon in *E. coli* excessive accumulation of proteins causes irreversible changes in host cellular homeostasis which cannot be restored by means of pathway and regulatory oscillations.[11–12]

For production of L-Dopa the strategies mentioned above and their related problems have been grossly observed and discussed by researchers. Munoz et al. reported improvement of L-Dopa production in *E. coli* by replacement of functional PTS system with over expression of galactose permease (GalP) and glucokinase (Glk) and deletion of transcriptional regulator tyrR which led to higher yield of aromatics. 4-hydroxyphenylacetate 3-hydroxylase (hpaBC) from *E. coli*, cyclohexadienyl dehydrogenase (tyrC) and chorismate mutase ($pheA_{CM}$) from *Zymomonas mobilis* were over expressed under IPTG inducible "trc" promoter. A feedback-resistant version of DAHP synthase (aroG) and *tktA* encoding transketolase, both from *E. coli* were also over expressed from a separate plasmid module. The final strains lead to a maximum titer of 1.5 g/L of L-Dopa in fermenter after 40-hr production phase.[13] Recently Wei et al. reported 8.67 g/L of L-Dopa by knocking out glucose-6-phosphate dehydrogenase gene (*zwf*), prephenate dehydratase and its leader peptide sequence (*pheLA*), transcriptional regulators (tyrosine repressor *tyrR* and carbon storage regulator A *csrA*) and switching glucose transport from the phosphotransferase system (PTS) to ATP-dependent uptake by over expression of galactose permease (*galP*) and glucokinase (*glk*). Multiplex automated genome engineering (MAGE) was used to improve L-Dopa production and the best strain after 40 hr of fed batch study yielded 8.67 g/L of L-Dopa. The fermentation medium (pH 7.0) contained 10 g/L of peptone and 5 g/L of yeast extract while the gross composition of feed was 500 g/L of glucose, 25 g/L of tryptone, 50 g/L of yeast extract, 17.2 g/L of $MgSO_4 \cdot 7H_2O$, 7.5 g/L of $(NH_4)SO_4$ and 18 g/L of ascorbic acid. Thus, a highly rich composition of media had been used which itself may contains a heavy stock of tyrosine/tyrosine precursors. Thus it is subtly impossible to obtain actual L-Dopa titers converted from tyrosine synthesized by the strain from

tyrosine stocks already present in Yeast Extract and Peptone. Furthermore, the study also includes over expression of hpaBC from plasmid under an inducible promoter.[14]

Three major control modals which have been universally accepted, reported and targeted by all authors as the primary determinants of regulation in the aromatic amino-acid pathway are tyrR gene which is involved in transcriptional repression of aromatic amino-acid biosynthesis and transport, feedback regulation of 3-deoxy- D -arabino-heptulosonate (DAHP) synthase (aroG) by phenylalanine and rate limiting pathway enzymes encoded by aroL or aroK. tyrR modulates expression of at least 8 unlinked operons. Seven of these operons are regulated in response to changes in the concentration of the three aromatic amino acids (phenylalanine, tyrosine and tryptophan). These amino acids are suggested to act as co-effectors which bind to the tyrR protein to form an active regulatory protein. Thus tyrR was deleted in our current study to increase the production of tyrosine which is a precursor to L-Dopa. Incorporation of feedback deregulated version of 3-deoxy-D-arabino-heptulosonate (DAHP) synthase (aroG*) gene by replacing wild type aroG, enhancing the expression of aroL and feedback deregulated tyrosine synthase (tyrA*) increased L-Dopa titers obtained from glycerol in this study. aroG converts 80% of the total DAHP synthesized from PEP and E4P to drive synthesis of aromatic amino acid in *E. coli*. aroG is highly sensitive to traces of phenylalanine that causes feed inhibition of DAHP synthase. Improvement of glucose transport by over expressing phosphoenolpyruvate synthase (PpsA) and transketolase A (TktA) to increase E4P supply for aromatic amino-acid synthesis has been reported to be partially effective and hence was not a part of this study. All these simultaneous modifications when taken together, however, did not translate in high L-Dopa productivity from glucose or glycerol unlike other metabolites like Shikimate, phenylalanine etc. Increasing copy numbers of pathway enzymes, fine tuning of RBS, intergenic region engineering, and enhancing RNA stability are some of the major strategies in metabolic engineering and have been targeted widely by researchers in developing high aromatic amino-acid producing bugs.[15] In the course of our study we realized that the key to extended production phases ultimately depend on flux balancing. High productivity relies mainly on an uninterrupted flow of flux maintaining a global steady state of the cell.[16] In this regard Juminaga et al. designed pathway modules for tyrosine over production in *E. coli*. The bio-brick operons were constructed in two different plasmid modules and they were ultimately transformed in *E. coli* MG1655 strain. The final strain was tested in fermenter and the plasmid modules were induced by IPTG to achieve higher expression of 10 pathway enzymes constructed in two plasmids to obtain 2 g/L of tyrosine from fed batch fermentation.[17] Thus all major works in this area had fundamentally been focused on higher expression of pathway enzyme rather achieving steady-state fluxes vital for extended phase of production.[18–19] More over as will be subsequently observed in the result section over expression of enzymes is ultimately associated with more acetate generation which undermines cellular health in long hours of fermentation.[20] High levels of protein inside the cell can trigger cellular stress response which summarily can hinder metabolite production.[21] In our current study to achieve the goal of having balanced flux minimum required modifications were assembled for synthesis of shikimate from glycerol rather than glucose in *E. coli* W3110 host genome and connections to other non-essential competing pathways diverting from E4P-PEP junction were removed. From Shikimate to L-Dopa-the synthetic pathway was constructed using two plasmids modules encoding total six genes. The modules were assembled in the engineered W3110 host and were tested for production. The promoters in the plasmid were used as constitutive with no IPTG induction and fed batch fermentation was performed using optimized feeding strategies with glycerol as the carbon source. The leaky expression of the promoters provided enough catalytic protein which leads to enhanced L-Dopa productivity in shake flasks. Fed batch fermentation of the best performer was run for 48 hr using a 2.5 L broth using modified minimal media containing 2% yeast extracts with a highest yield of 12.5 g/L of L-Dopa for an exponential feeding profile.

Materials and method

Details of cloning procedures and genome modifications

The base plasmid used in this work was pMALp2X from NEB. pY3 (https://www.addgene.org/50606/) and pS3 (https://www.addgene.org/50596/) plasmids with their constructs[17] were kindly donated by Prof. Jay Keasling, Lawrence Barkley National Laboratory. Both pRBS1, the base plasmid for pY3 and pMALp2X have ampicillin resistance as a selection marker. The ampicillin resistant gene in pMALp2X was inactivated by inserting kanamycin resistance cassette (from pET29a plasmid) in the unique *Sca*I restriction site present within coding sequence of the amp gene, the vector so forth was called pMAL-Kan. The Dopa module converting tyrosine to L-Dopa called as pMAL-Kan + HpaBC (CS1) was constructed by cloning hpaBC gene [4-hydroxyphenylacetate-3-hydrolase] which was PCR amplified from BL-21DE3 *E. coli* strain (Fig. S1 in Supplementary Material) between *Nde*I and *Eco*RI restriction sites. The 5′-UTR region upstream to hpaC was used in its native form. Choice of restriction sites *Nde*I and *Eco*RI automatically excised the maltose binding fusion protein downstream to the promoter in pMALp2X vector. In another construct pMAL-Kan + HpaBC + aroG* (CS2), feedback resistant aroG* gene (amplified from the pS3 plasmid) with a consensus ribosomal binding site of 5′-AGGAGG-3′ and spacer sequence of 5′-CCATCC-3′[22] was cloned between *Eco*RI and *Xba*I restriction sites (Fig. 2). tyrR (transcription regulator), pykF (gene responsible for directing the PEP flux toward pyruvate to super pathway of Valine family amino-acid synthesis) and serA (gene responsible for directing glycerate-3-phosphate flux toward super family of Histidine amino-acid biosynthesis) were deleted from wild-type *E. coli* W3110 by P1 transduction [Details of lysate preparation and

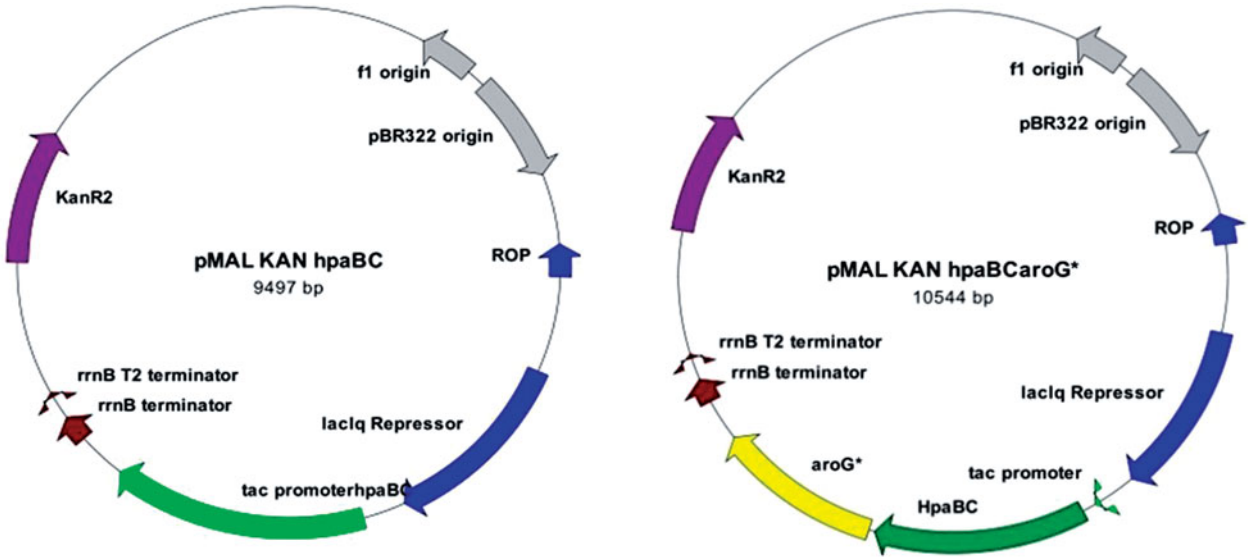

Figure 2. pMAL–KAN hpaBC (CS1) and pMAL–KAN hpaBC aroG* (CS2) were used as Dopa module in combination with plasmid pY3 in modified strains A and B.

calculation of phage titer available in Section 4.2] employing method described by Thomason et al. and hence was designated as Strain A.[23] The corresponding donor mutants for performing transduction were purchased from *E. coli* Genetic Resources at Yale CGSC (http://cgsc2.biology.yale.edu/), as shown in Table 1. The plasmid pCP20 (replicates only at 30 °C or below) which had a heat sensitive origin of replication and express FLP recombinase at high temperatures (37 °C and above) (https://cgsc2.biology.yale.edu/Site.php?ID=64621) was used to remove the kanamycin cassette inserted while performing transduction as selection marker.[24] (Fig. S2 in Supplementary Material confirms the removal of kanamycin cassette after the deletion of tyrR gene by FLP recombination.).

Furthermore, Strain B was constructed by knocking in aroG* (gene encoding feedback deregulated DAHP synthase, Figs. S3 and S4 in Supplementary Material confirm the integration of aroG* with chloramphenicol cassette and successful removal of chloramphenicol cassette.) in the *E. coli* W3110 strain as described by Tyagi et al.[25] along with all other modifications mentioned before. Strain A was designated S1 after the transformation of CS2 and pY3 plasmids while Strain B was transformed with CS1 and pY3 plasmids and hence so forth called Strain S2. The third combination of only *E. coli* W3110 transformed with CS1/CS2 and pY3 were used as controls and were called C1 and C2, respectively (Table 2). The lists of the primers, plasmids and the mutants and their applications have been summarized in Tables 3 and 4.

Table 1. List of strains used to transfer deletions in *Escherichia coli* W3110.

Name of the donor strain	Mutated gene	Selection cassette
tyrR760(del)::kan	tyrR transcriptional regulator	Kanamycin
serA764(del)::kan	serA L-serine biosynth pathway	Kanamycin
talA784(del)::kan	talA sedoheptulose pathway	Kanamycin
pheA762(del)::kan	pheA phenylalanine biosynthesis	Kanamycin
pykF751(del)::kan	pykF pyruvate synthesis	Kanamycin

HPLC analysis

HPLC analysis was performed using an Agilent 1260 Infinity Series HPLC system equipped with PDA detector and Refractive index detector (RID). Agilent ZORBAX Analytical Eclipse Plus C18 (4.6 mm × 150 mm, 5 µm) column was used for L-Dopa, Tyrosine analysis at 280-nm wavelength with a flow rate of 0.5 mL/min. The separation was optimized using gradient flow of two simultaneous buffers. Buffer A was water, methanol, and acetic acid in 80:19:1 ratio with final pH being 2. Buffer B was 70% methanol and water.[26] Glycerol and acetate were separated and estimated using Aminex Column from BioRad. 5-mM sulfuric acid was used as isocratic buffer for separation. Acetate was detected and quantified at 210-nm wavelength using PDA. Glycerol estimation was performed by RID simultaneously.

GC–MS analysis

For targeted metabolite detection and quantification GC–MS analysis of broth supernatant were performed. High-purity analytical grade L-Dopa, tyrosine, pyruvate, and Shikimate were purchased from Sigma and Hi-Media. The broth supernatants were filtered using 0.2-µM syringe filters and 500 µL were lyophilized in 2 mL amber glass GC vials. To the dried residues 50 µL of 2 mM methoxylamine in pyridine was added and incubated at 37 °C for 1 hr to block keto functionalities in metabolites by oxime formation. Finally a neat aliquot of 100 µL BSTFA was added to the sample and incubated at 60 °C for 1 hr. 1 µL of the derivatized sample was injected and analyzed in Shimadzu QP-2010 Plus GC with Thermal Desorption System TD 20 Gas Chromatograph Mass Spectrometer. The observed peaks were matched to compounds using NIST metabolic library. The mixture of the metabolite standards was treated similarly.[27]

Table 2. Details of strains and plasmid combinations used in this study.

Basic strain	Modified strain	Genomic level modifications	Plasmid modules incorporated		Final strain
W3110	Strain A	Δ*pyk*F Δ*tyr*R Δ*ser***A**	pY3	CS2	S1
W3110	Strain B	Δ*pyk*F Δ*tyr*R Δ*ser***A** *aroG*^{fbr}	pY3	CS1	S2
W3110	C1	No	pY3	CS1	C1
W3110	C2	No	pY3	CS2	C2

Table 3. List of important primers used in this study.

Serial no.	Name of primers	Sequence	Application	Reference
1	hpaBC forward	CATATGAAACCAGAAGATTTCCGCGCCAG	Cloning of hpaBC gene.	Current study
	hpaBC reverse	GAATTCTTAAATCGCAGCTTCCATTTCC		
2	Pet kan forward	AAAACTCACGTTAAGGGATT	Insertion of kanamycin gene in pMAL P2X Vector	Current study
	Pet kan reverse	ATTTAACGCGAATTTTAACAAAAT		
3	aroG knockin forward	ATTGGAAGTATTGCATTCACTAAGATAAGTA-TGGCAACACTGGAACAGACATGAATTAT-CAGAACGACA	Knockin of aroG* in place of native aroG gene.	Tyagi et al.[25]
	aroG knockin reverse	TGGTGATTCATCGGATACGCCACTCTGACG-GCGCATCCGACAATTAAACCATGGGAAT-TAGCCATGGTCC		
4	aroG knockin confirmation forward	TCCAGGATTAATCCGTTC	Confirmation of aroG* gene knockin.	Tyagi et al.[25]
	aroG knockin confirmation reverse	GAGTCGGCTTTTTTGTTG		
5	tyrR deletion confirmation forward	TGCCCGTTTTTCCGTCTT	Confirmation of tyrR gene deletion.	Tyagi et al.[25]
	tyrR deletion confirmation reverse	GATGAAATCACCACCGAG		
6	pykF confirmation forward	GGGGTACCTGTCTAACAAGTTG	Confirmation of pykF gene deletion.	Current study
	pykF confirmation reverse	CGGGATCCGACAGTCTTAGTCTTT		
7	serA confirmation forward	TCGCGACGCAAACGTTCATAT	Confirmation of serA gene deletion.	Current study
	serA confirmation reverse	AGACTCGCAAAGTAGAATGCG		

Table 4. List of plasmid constructs used in this study.

Serial no.	Name of the plasmid	Application in current study	Selection markers and "Ori"	Genes cloned
1.	pMAL P2X New England Biolabs	Dopa Module	Ampicillin, pBR322-ori-F	Promoter: tac hpaBC
2.	pMAL p2X KAN	Dopa Module	Kanamycin, pBR322-ori-F	Promoter: tac hpaBC, aroG*
3.	pY3 Vector Backbone: pRBS-01,[17]	Tyrosine Module	Ampicillin, p15a	Promoter: lacUV5 tyrB, tyrA, aroC Promoter: pTRC aroA, aroL
4.	pKD46, Dr. Jean Pierre Hernalsteens, Belgium	Ap, λ Red recombinase expression	https://cgsc2.biology.yale.edu/Site.php?ID =64672	–
5.	pCP20, Dr. Jean Pierre Hernalsteens, Belgium	ApCm, FLP recombinase expression	http://cgsc2.biology.yale.edu/Site.php?ID =64621	–
6.	pUCaroG^{fbr}chl,[25]	Cloning of the *aroG*^{fbr} with chlor cassette	Ampicillin	pUCaroG^{fbr}chl

Carbon-dioxide estimation

We need to look at the precise distribution of various glycerol fluxes in different hours of fermentation. Therefore, carbon dioxide measurement was critical. The concentration of carbon dioxide in exit gas was measured in percentage using an Ametek DYCOR process mass. The process mass spectrometer was previously calibrated with varying argon concentration.

Media

Modified minimal media was used for all cell cultures except otherwise mentioned. With all the mentioned modification assembled under *E. coli* W3110 chassis, it was observed that in minimal media the growth of the final strain is compromised. Although a number of parameters can be considered during media design, the experiments and their outcomes will be fairly large and uncertain. The following puzzle was solved by supplementation of yeast extract as potential source of amino acids and vital micro-nutrients to assist growth initially. The following recipe gave us the best result:

Media composition

Sodium citrate (2.4 g/L), NaCl (2 g/L), $MgSO_4$ (1 g/L), NH_4Cl (2.5 g/L), K_2HPO_4 (3 g/L), $FeSO_4$ (200 μM), Vitamin C (4 g/L), thiamine (0.1 g/L), pyridoxine hydrochloride (0.1 g/L), yeast extract (2 g/L), peptone (2 g/L), glycerol (25 g/L) and trace metal solution (1X) (see Section 4.1.3 for justification of addition of 2 g/L of yeast extract and peptone).

Trace metal composition

100X consists of $CaCl_2$ (1.5 mg/L), $ZnSO_4$ (12 mg/L), H_3BO_3 (3 mg/L), $CuCl_2.4H_2O$ (2 mg/L), $MnCl_2.4H_2O$ (15 mg/L), $CoCl_2.6H_2O$ (2.5 mg/L), $Na_2MoO_4.2H_2O$ (2.5 mg/L), and EDTA (5 mg/L). Iron was found to be a limiting nutrient and L-Dopa production depends on adequate Fe^{2+} supply.[28] Wei et al. reported addition of peptone up to 10 g/L,

Table 5. Parameters of fermentation.

Fermentation parameters	Description of settings
Temperature	37 °C
pH	Set points 7, 1(N) HCl and 4% ammonia solution were used in acid and base pumps, respectively, to adjust pH automatically.
Dissolved oxygen (DO)	Overnight agitated sterilized media was set at 100% DO enriched. Minimum set point value for DO was 40%.
Agitation	Cascaded with DO up to 1200 RPM. 0.3–0.5% O_2 enrichment was necessary after OD value reached 25 and onwards. After 28 hr O_2 enrichment was stopped due to higher DO values.
Feed	Composition of feed: 2% yeast extract, 40% glycerol. For normal constant fed batch fermentation initial feed rate was 15 mL/hr. For exponential feeding the rates were 15 mL/hr, 17.835 mL/hr, 21.21 mL/hr, 30 mL/hr.
Broth volume	Initially 2.5 liters final 4.0 liters (approx).

yeast extract up to 5 g/L in their modified media composition and up to 50 g/L of yeast extract, and 25 g/L of peptone in feed for production of L-Dopa in bioreactor. In contrast, our designed media contains very less yeast extract and the possibility of L-Dopa produced from existing tyrosine stock in yeast extract is negligible. It is to be noted that no component of yeast extract have corresponding peak at 280 nm at the retention time of L-Dopa (5.1 min) in HPLC profile. This was verified by blank media profiles using same HPLC method used to quantify L-Dopa.

Fermentation optimization

Fermentation optimization is very crucial in metabolic engineering as it provides a closer look at various fluxes. Even qualitative analysis of fluxes can provide vital insight to decouple various parameters involved in production, e.g., growth, CO_2 production, substrate consumption, product formation. Different feeding strategies can be optimized having a closer look at the CO_2 production rates, acid production and residual substrate levels at different hours of fermentation. The studies were performed in New Brunswick BioFlo® 310 fermenter with a vessel capacity of 5.0 liters. The bioprocess studies were performed in fed batch mode. A single colony from agar plate were picked up and inoculated in LB containing antibiotic ampicilin and kanamycin to obtain primary culture. The primary culture was used to inoculate 250 mL secondary culture having media composition described in Section 2.4 with the mentioned antibiotics and grown overnight. An inoculum size of 10% of the total media volume in the fermenter was used for seeding. The fermentation parameters are summarized in the Table 5.

Result and discussion

Shikimate pulse experiment

To establish that the pY3 and Dopa module together can channelize major shikimate flux toward L-Dopa a shikimate pulse experiment was designed where five flasks including a control were inoculated with wild type W3110 strain

Table 6. Details of shikimate pulse experiment.

Flask no.	Concentration of shikimate in pulse	Interval of pulsing/total no. of pulses
Shik C	No pulse	–
Shik 1	0.1 gm/L	2 hr/5
Shik 2	0.2 gm/L	2 hr/5
Shik 3	0.5 gm/L	2 hr/5

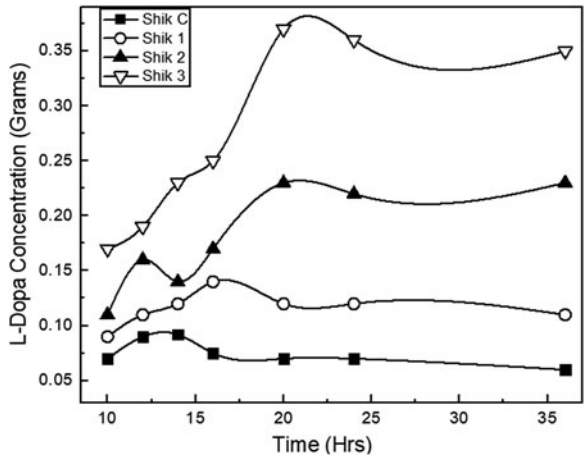

Figure 3. Product profiles for L-Dopa due to different concentrations of shikimate pulsed.

carrying the two plasmid pathway modules (Strain C1) in LB media. Different concentration of shikimate pulses were given to all the flasks after 6 hr of inoculation when the cells were in mid-log phases against a control which was not pulsed. The resulting supernatant was estimated for L-Dopa. Table 6 provides the details of shikimate pulsing. From the pulsing experiment, it was clear addition of shikimate pulses did increase L-Dopa productivity. Further addition of pulse above 0.5 g/L did not lead to any further improvement. The reason may be shikimate transporters either being saturated or in due course of metabolic slowdown of the cell. It is to be further mentioned that no induction was performed and the natural leaky expression from the promoters supplied enough catalytic proteins to shift Shikimate flux toward L-Dopa. However, due to metabolic stress and the media being LB the final ODs were only around 2.5 in all flasks. The two modules combined can thus divert major shikimate fluxes to L-Dopa under constitutive expression of the promoters harbored in the pathway modules, as shown in Figure 3.

Shake flask studies

Shake flask studies were performed using Strain A and B transformed with plasmids CS2 and CS1 consecutively and Y3 construct. All shake flask studies were performed using media recipe described in Section 2.4. However, glycerol and glucose as carbon source were used and compared for the production. The pH readings were obtained at different time intervals along with optical density to check acid production with time.

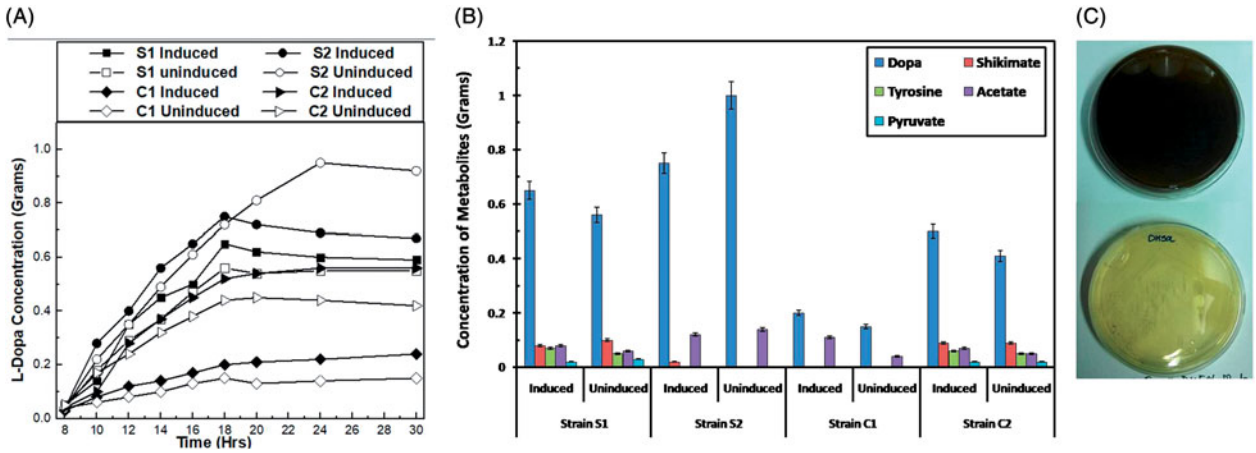

Figure 4. (A) Production profiles of L-Dopa in different strains. Uninduced S2 cultures with low production rates but longer production phases translated into higher titers of L-Dopa than induced cultures of S2. (B) Targeted metabolite analyses showed S2 cultures both induced and uninduced had no tyrosine or pyruvate accumulation unlike both induced and uninduced S1 cultures. (C) S2 strain streaked on a normal Luria Agar plate after 36 hr in contrast to a normal Luria Agar plate streaked with *Escherichia coli* DH5α strain.

L-Dopa production under induced/uninduced systems

All constructed combinations were studied individually with and without induction. It was observed that there was significant level of L-Dopa accumulation in S1 and S2 cultures. However, the levels of L-Dopa were higher for S2 across all evaluated assemblies after 24 hr under induced and uninduced condition. Productivities of the top performer S2 and S1 were analyzed under induction (Fig. 4A). The broth of the induced culture was less dark in color for S1 compared to S2 (darkening of the culture, because of the protein expression and activity coded by hpaBC gene) and there was less L-Dopa accumulation. Performing induction should have translated into higher levels of protein buildup inside the cell including that of 4-hydroxyphenylacetate-3-hydrolase but this has not added any further improvement in production of L-Dopa. The plausible reason behind the observation was realized when pntAB (NAD (P) transdehydrogenase) and DDC genes (aromatic amino-acid decarboxylase) were cloned downstream to the hpaBC gene to further improve L-Dopa production and for extending the final product up to dopamine in separate experiments. In both the cases, the expression of hpaBC was downregulated resulting in development of very light brown color compared to intense browning for S2 on Luria Agar plates and development of light band for hpaB expression in SDS PAGE. The fact that because S1 actually contained aroG* cloned downstream to the hpaBC in CS2, this might have hampered hpaBC expression like observed before, thereby leading to only partial conversion of tyrosine into L-Dopa. If the CS2 construct was reversed, i.e., aroG* cloned directly after "tac" promoter followed by hpaBC downstream the browning of the plates became even lesser. So obviously only hpaBC in CS1 proved to be the best option. Possible explanation of the observed result may be the stability of the polycistronic mRNA and probable inhibition of translation due to mRNA secondary structures.[29–30] Targeted metabolite analysis (Fig. 4B) revealed that S2 contained almost negligible amount of Shikimate, pyruvate and most importantly no tyrosine but there was acetate accumulation in all broths. Thus, our observation strongly contrasts that of Wei et al. where PHAH is indicated as the rate-limiting enzyme for L-DOPA biosynthesis in this strain. However, S1 broth strikingly contained a fair amount of Shikimate very less pyruvate and even tyrosine. If both S1 and S2 were induced there is actually a spike in increase in L-Dopa production which continued for 10–12 hr after induction but eventually flattened out in both the cases. However, the induced cultures of S2 were darker in color than uninduced cultures but actually contained less L-Dopa. It is important to note that the enzyme 4-hydroxyphenylacetate-3-hydrolase is a robust enzyme having a broad spectrum of aromatic substrates. Increased enzyme levels also lead to a greater no. of other byproducts.[31–32] In the constitutive system where there was no induction, production from S2 sustained for 20 hr producing higher titer values of L-Dopa. L-Dopa titers obtained from C2 induced were somewhat comparable with titers obtained from S1 but for C1 no significant titers of L-Dopa were obtained. This confirms incorporation of feedback deregulated aroG* is crucial to obtain higher titers of L-Dopa. The amounts of phenylalanine present in yeast extract can feedback regulate wild type DAHP (aroG) activity. The better performer S2 was hence selected for further studies. The slow production of L-Dopa on plate can be observed by the intense browning developed on Luria agar plates (Fig. 4C) in due course of time. Furthermore, the better performance of S2 under uninduced condition of Luria agar plates testifies the result obtained in liquid broth. Table 7 shows best titers of L-Dopa obtained using different conditions and assemblies.

Analysis of acetate generation depending on carbon source

Acetic-acid generation is one of the major problems encountered during production of aromatic amino acid. In fact, acetic-acid generation leads to drop in pH, affects cellular health and is a major issue in long hours of fermentations. Glucose, glycerol, and combination of glucose + glycerol

Table 7. List of maximum titers of L-Dopa obtained from different assemblies and conditions.

Strain (base strain W3110)	Genomic modifications	Plasmid module	Media and condition	Final L-Dopa titer in gm/L
C1	No	CS1 and pY3	LB and shikimate pulse of 0.5 gm/L	0.35
C1	No	CS1 and pY3	Modified minimal, induced	0.22
C2	No	CS2 and pY3	Modified minimal, induced	0.44
S1	Δtyr ΔpykF ΔserA	CS2 and pY3	Modified minimal, induced	0.55
S2	Δtyr ΔpykF ΔserA aroG*	CS1 and pY3	Modified minimal, uninduced	0.95

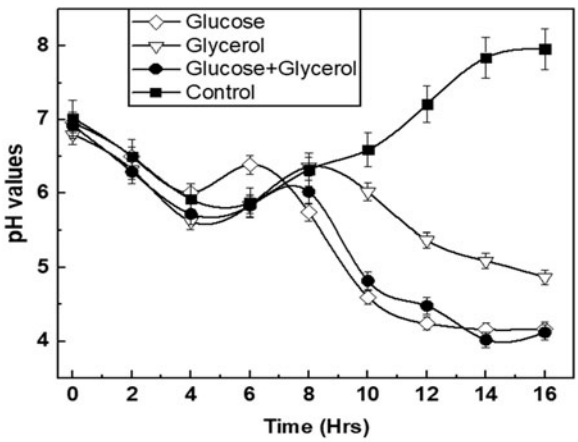

Figure 5. pH profiles at different hours in shake flask depending on different carbon sources used.

were tested as viable carbon source for L-Dopa production against a control with no glucose and glycerol and their marked effect on acetate generation during L-Dopa production were observed under uninduced condition. L-Dopa production was slightly better if glycerol was used as a carbon source over glucose. However, there was fairly marked effect on acetate generation and pH drop in cultures. It was observed that for glucose pH dropped up to 4.2; however, for glycerol the final pH was around 5.3 (Fig. 5). In fact, the steady drop in pH may be the plausible reason behind reduced L-Dopa production when glucose was used as carbon source. The trend in pH drop was same as that of glucose when glucose + glycerol were the carbon source. The results question the utility of glucose as a carbon source for metabolite over production. Bren et al. reported that glucose is a very poor source of carbon in presence of glutamate, arginine, and proline because of reversed diauxic shift that retard growth and increase acid production. The reversed diauxic shift has been attributed to imbalance in carbon nitrogen ratio that results in higher levels of α-keto glutarate and declining cAMP levels.[33–34] Since the media contains arginine, glutamate, proline due to addition of yeast extract and peptone glucose turned up to be a poor source of carbon in our current study. Hence, by switching from glucose to glycerol production is not affected but has certain impact on pH drop observed in this study. Most of the current literatures in metabolic engineering for metabolite production report the use of glucose. However, glycerol can also be a better carbon source for metabolite production and to put it more precisely glycerol actually turned out to be a better choice as carbon source for L-Dopa production for our engineered strain.

L-Dopa production study in fermenter

During first 8 hr of inoculation no significant product formation was observed. There were no major changes in exit gas CO_2 levels, pH, and optical density. Expression of all the promoters in the two plasmid modules carried by host were constitutive during fed batch analysis. The product profile and logarithm of optical density are shown in Figure 6A. The figure demonstrates similar trends of biomass and product formation. However, observing the kinetics of product, CO_2, and acid formation provided a contrasting picture. It was observed that L-Dopa production started actually from 8th hr onwards and production rate increased at two different phases. This was between 8–10 hr and 14–16 hr after inoculation Figure 6B. From the OD_{600} plot a closer look revealed a striking similarity between these two time points – in both these points the growth rate was slow. However, between 10 and 14 hr there had been steady increase in growth but product formation rate declined. These observations were confirmed from the levels of CO_2 in the exit gas (Fig. 6B). Between 8th and 10th hr CO_2 production rate increased along with increase in rate of product formation. This was largely due to high metabolic activity and the cells producing biomass in nutrient rich media. This phase of production was growth associated. During 14–16 hr the CO_2 production rate had dipped continuously as growth slows down further but after 16th hr the CO_2 production rate increased up to 20th hr. This part of production was largely decoupled from growth. However, the increase in rate of CO_2 production ascertained that this phase of production was not growth dependent and further the increase in rate of CO_2 production was associated to meet the requirement of ATP and NADH. Looking at the acetic-acid profile (Fig. 6B) it was clear that acid production rate had been higher during growth phase but eventually fell as growth slowed down. Hence, L-Dopa production or the aromatic amino-acid biosynthesis super pathway functioning and acid productions were not necessarily coupled. Literature survey revealed that acetate generation had been reported during aromatic amino-acid synthesis in engineered strains. However, such studies were based on use of glucose for synthesis of aromatic amino acid and L-Dopa but glycerol instead was used in current study. It had already been observed that in shake flask glycerol as carbon source led to lower acid generation when compared with glucose. Furthermore, acetate generation profiles were co-terminus with protein synthesis during growth phase. Looking at various glycerol fluxes during different hours (Fig. 6C) (see Section 4.1for the calculation of fluxes qualitatively in terms of grams of glycerol equivalent from HPLC data) it was

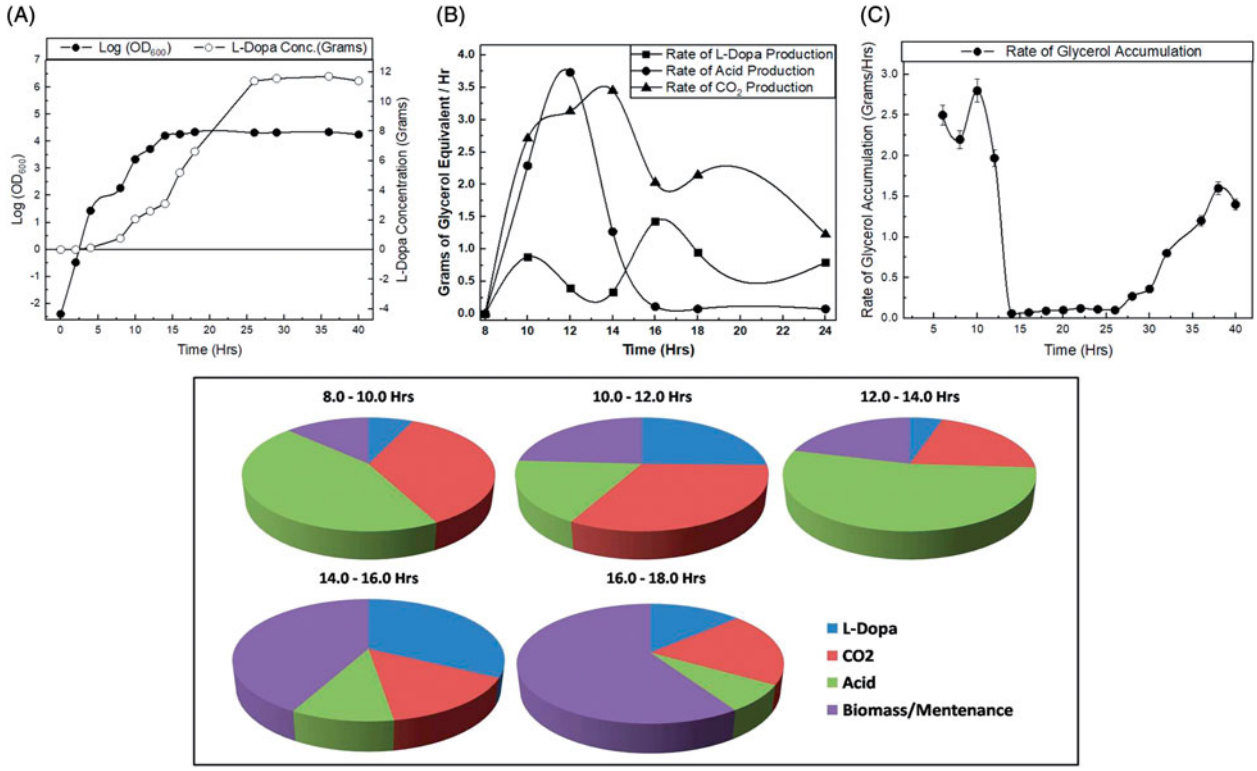

Figure 6. (A) Log (OD) and product profile for constant feeding batch cultivation of strain S2. (B) Rate profiles of product, CO_2 and acetic-acid formation. (C) Various glycerol fluxes during vital hours of fermentation. (D) Glycerol accumulation profiles for constant feeding.

observed that as L-Dopa production increased glycerol flux toward cellular requirement also increased but OD value remained constant. This large glycerol flux was probably directed toward cellular maintenance. Functioning of aromatic amino-acid biosynthesis has its own cost which, as earlier mentioned is highly energy intensive. Furthermore, up to 12th hr after inoculation the biomass generation sustained on nutrients from yeast extract and carbon from glycerol. But after 12th hr of inoculation due to minimum supply of yeast extract through feed biomass and maintenance were completely shifted to only available carbon source glycerol. This was observed from the fact that a large flux of glycerol was directed for biomass generation and cellular maintenance during 16th and 18th hr. This also indirectly confirmed that L-Dopa was being produced from tyrosine synthesized from aromatic amino-acid pathway itself rather than from tyrosine inventory of yeast extract. Estimation of residual glycerol (Fig. 6D) revealed that actually there was little glycerol left in the broth between 15th and 27th hr. This was in agreement with the trends observed from flux. Glycerol uptake was almost 100% between up to 27th hr. After this glycerol levels slowly built up as cells were not able to consume glycerol as efficiently as before. Now from 12th hr to 27th hr glycerol accumulation had been significantly less even though growth already ceased after 20th hr. Hence effectively the production after 20th hr was not growth associated. From 20th hr to up to 36th hr 5 g/L of L-Dopa had been produced that is almost 40% of the total production. The final titer of L-Dopa obtained from the broth after 40 h was 11.37 g/L from constant feeding profile.

Exponential feeding strategy

A closer look at the glycerol accumulation rate vs. time course profile provided hint of scope for further improvement in L-Dopa production. From 12th to almost 25th hr the rate of glycerol accumulation was negligible. Real-time analysis of the broth showed very little residual glycerol levels. Now this means that the cells were efficiently consuming glycerol added through the feed. We asked whether this uptake capacity can be pushed by further increasing feed rate. However, after 25th hr clearly it was useless to increase feed any further since glycerol was increasingly accumulated. But the original question turned out to be more complex as product formation rates were simultaneously observed. Now there were two distinct phases of production viz. growth associated phase, i.e., between 8 and 10 hr and growth independent phase, i.e., 14–16 hr. In both the phases rate of L-Dopa production had increased. So there were two plausible target phases where actually increasing glycerol supply can further enhance production. However, increasing supply of glycerol in the growth associated phase would lead to little improvement in terms of productivity, because carbon was primarily directed toward growth and bio-mass formation at this phase. In fact when glycerol supply was increased at this phase actually there was little improvement in L-Dopa production (data not shown). The second phase of production which was largely uncoupled from growth was targeted. It was decided to increase feed rate exponentially from an initial rate of 15–30 mL/hr from 12th hr to 18th hr and then decrease it back exponentially to again 15 mL/h from 18th to 28th hr. Immediately the effect of this

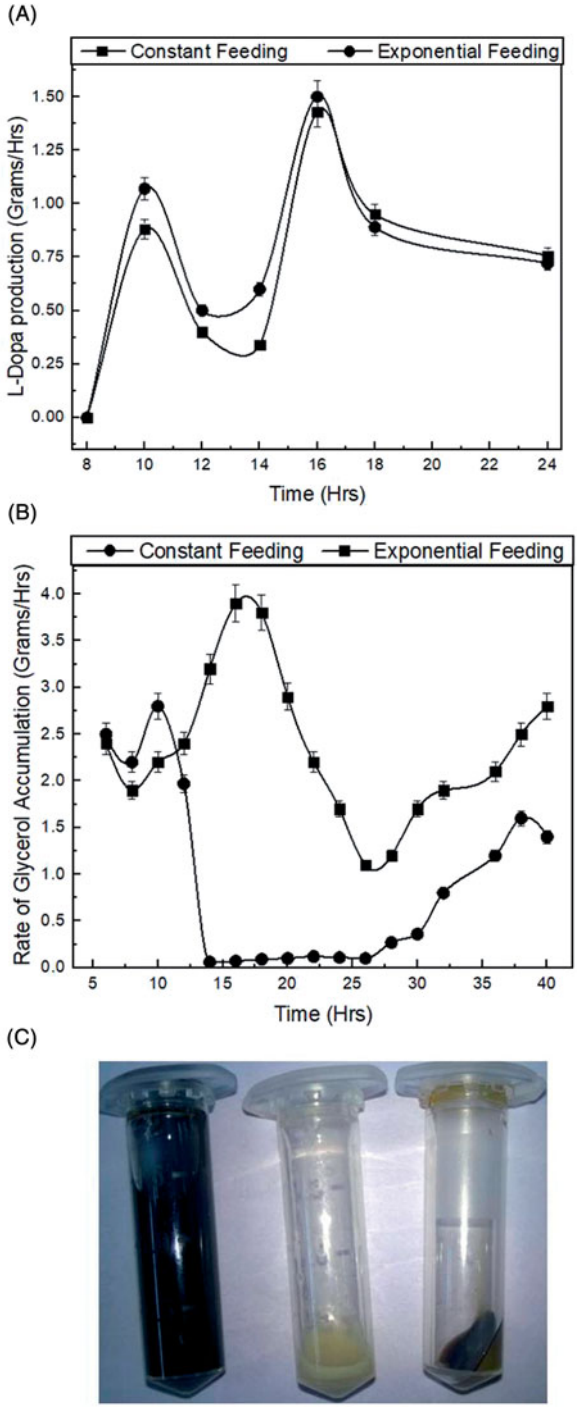

Figure 7. (A) Comparison of product formation rates for constant feeding and exponential feeding. (B) Comparison of glycerol accumulation profiles for constant feeding and exponential feeding. (C) Color of broth and pallet from pilot fermenter in contrast to normal *Escherichia coli* DH5α cell pellet.

strategy was manifested in enhancement of L-Dopa production rate in the second phase of production (Fig. 7A). Comparison between the two rates have been shown in through plots where clearly the rate of production had increased between 14th to 18th hr and there was a net 1.2 g/L gain in overall production of L-Dopa leading to a final titer of 12.5 g/L. No corresponding change in acid production rate was observed but there was increased CO_2 production. The residual glycerol level vs. time course profile (Fig. 7B) clearly shows the exponential feeding strategy had led to left over glycerol in the broth which implies that through exponential feeding sufficient amount of glycerol had been provided to the cells. Thus simple strategies looking at real-time trends of product profile, CO_2 generation can provide vital inputs for bio-process optimization of production without any further tedious modification of the host. In conjunction with minimum vital modifications that were assembled in host and with the help of highly maneuverable pathway modules it had been possible to enhance L-Dopa production by 40% from the last reported maximum titer. From (Fig. 7C) the extent of product formation is apparent from the intense color of the broth and the fermenter pellet which appears much deeper in color compared to normal *E. coli* DH5α cell pellet when a pilot scale bioreactor was run without addition of ascorbic acid.

Mathematical interlude

Calculation of fluxes in glycerol equivalent

In order to understand flux qualitatively different products are to be expressed in the same scale. To achieve this we have the following assumptions:

1. The nutrient in the initial broth was exhausted between 8 and 10 hr and product, biomass and CO_2 production is mainly from the carbon supplied through feed.
2. The feed contains 40% glycerol and is the only significant source of carbon.[35]

Calculation of L-Dopa and acetate fluxes in grams of glycerol equivalent

L-Dopa having nine carbon atoms with a molecular weight of 197 is synthesized from glycerol. Balancing the carbon atoms, 197 g of L-Dopa is obtained from 3 × 92g of glycerol (1 mole of glycerol ≡ 36 g of carbon ≡ 92 g of glycerol). Hence, $y = \frac{3\times 92}{197} \times x$, where x is the amount of L-Dopa in g and y is the glycerol equivalent (in g) of x g of L-Dopa.

Similarly, for acetate $z = \frac{2\times 92}{3\times 59} \times x$, where x is the amount of acetate in g and z is the glycerol equivalent of acetate. Similarly, other fluxes can be calculated in glycerol equivalent.

Calculation of CO_2 fluxes in grams of glycerol equivalent using process mass data

The process mass displays gas concentrations in percentage. At different hours of fermentation, the CO_2 concentration fluctuates. Hence, the % of CO_2 over a period of 1 hr is converted in moles or grams of CO_2, to be further converted into grams of glycerol equivalent:

Vessel volume = volume of media = 2 L.

Air flow rate = 2 L/min.

Vessel volume per minute (VVM) = 1; room temperature = 20 °C and pressure = 101 kPa

Under the following conditions, the volume of air can be approximated to 22.4 L.

1 VVM = 1/22.4 mole/min = 60/22.4 mole/hr. x is the average of % of CO_2 reading in process mass over a period of 1 hr.

Hence, $X\%\ CO_2 = \frac{x \times 2 \times 60}{100 \times 22.4}$ mole of CO_2/hr or $X\%\ CO_2 = \frac{x \times 2 \times 60 \times 44}{100 \times 22.4}$ g of CO_2/hr.

The following can be converted to CO_2 into glycerol equivalent using arguments in Section 4.1.1.

Calculation of amino-acid requirements for cell

The average abundance of a particular amino-acid molecule in *E. coli* per cell is roughly 3×10^8. The maximum OD obtained for the engineered strain under fed batch fermentation was around 50. Hence, the total number of molecules of an amino acid required for 50 OD culture is roughly $3 \times 10^8 \times 50 \times 10^8 = 15 \times 10^{17} \equiv 2.5 \times 10^{-6}$ moles. This can be compared with aspartic acid content of 1 g yeast extract $= 2 \times 10^{-4}$ moles.[36] Thus, supplementation of 2 g of yeast extract and peptone should be sufficient to assist initial requirements for growth. A table (STAB 1) has been further provided in supplementary section data section for reference to other amino acids in yeast extract.

(Source: http://www.tekniscience.com/documents/Yeast_Extract-19512.pdf)

Calculations of titer value of P1 phage

The experimental protocol described by Thomason et al. was followed for performing P1 transduction. As suggested by the authors, the plate method yields higher titers than the liquid culture method. However, titer values of phage should always be calculated before starting any experiment. We observed and obtained titer values over 10^{11} regularly using plate method. To obtain higher titer values, we prepared a series of dilution of the stock in geometric progression ranging from 10^2 to 10^8. Each dilution was spotted (10 µL) on LA plates supplemented with Ca^{2+} developing a smooth lawn of bacteria after overnight incubation. The highest dilution having no. of discrete small plaques over a small area were counted and were used for the calculation of titer:

$$\text{Titre value (per mL)} = \frac{\text{No. of counted plaques} \times 10^{x} \times 1000}{\mu\text{L of dilution used for spotting}},$$

where x are folds of dilution.

For a dilution of 10^8 when spotted with 10 µL, a titer value of 10^{11} can be obtained. When titer value drops below 10^9, the chances of transduction is drastically reduced.

Conclusion

The study focused on achieving higher titers of L-Dopa through minimum modification of the host. Thus, the focus was on achieving higher fluxes toward product formation with minimum perturbation of host-cell steady state. For metabolite over production, the general approach to divert major metabolic flux toward a particular pathway by making higher levels of catalytic protein is not universal. Though for synthesis of open chain highly oxidized compounds like shikimate, this is often a fruitful strategy but for aromatic amino-acid synthesis owing to their higher demand of molecular resources like ATP and NADH steady-state and host-cell physiology is compromised. Thus, the strategy to increase flux antagonizes the resources required for the enhancement of flux. We observed such strategies leads to product formation to occur in short bursts, but is not sustainable for long production phases. From the current study it was observed that for L-Dopa long hours of sustained fermentation even when the production rate was low can be beneficial because the ultimate titers obtained was higher. In shake flask studies, culture S2 without induction performed better in terms of final titer. Hence, slow production rates with balanced flux often translates into better production. It was observed from our work that glycerol is a better carbon source compared to glucose for metabolite over production particularly when production phases were shifted to only carbon source added through feed. Further imbalance in nitrogen/carbon ratio led to reverse diauxic effect which in turn led to higher acetate generation when glucose was used as a carbon source. When glycerol was used as a carbon source the production of L-Dopa for the engineered strain had two distinct phases viz. growth associated and growth independent phase. Increasing supply of carbon in growth independent phase through exponential feeding led to increase in L-Dopa titer. It was observed that production of L-Dopa was not associated with simultaneous generation of acetate. Rather it was synthesis of protein that was coterminus with acetate generation in log phase. This is contrasting to our general idea of functioning of the energy intensive L-aromatic amino-acid pathway. However, it cannot be altogether denied that protein levels have a critical role in flux diversion. It is still largely an unaddressed field that what should be the highest upper limit of different protein levels in a pathway that is vital for flux diversion, beyond which increasing protein levels will lead to deleterious effects on cellular physiology which will ultimately hamper production.

Acknowledgments

The authors are highly grateful to Prof. Jay D. Keasling who is a Professor of Chemical Engineering and Bioengineering at the University of California, Berkeley for kindly providing us the pY3 and pS4 plasmids with their constructs which were used in this study.

Funding

The authors acknowledge DBT Builder Project, JNU funded by Department of Biotechnology, Govt. of India for providing instrumentation and facilities.

References

[1] Simuni, T.; Hurtig, H. Levodopa: A Pharmacologic Miracle Four Decades Later. In *Parkinson's Disease-Diagnosis and Clinical Management*. Factor S., Weiner W., Eds; Demos: New York, 2008; pp. 471–490.

[2] Min, K.; Park, K.; Park, D.-H.; Yoo, Y.J. Overview on the Biotechnological Production of L-DOPA. *Appl. Microbiol. Biotechnol.* **2015**, *99*, 575–584.

[3] Knowles, W.S. Asymmetric Hydrogenation. *Acc. Chem. Res.* **1983**, *16*, 106–112.
[4] Koyanagi, T.; Katayama, T.; Suzuki, H.; Nakazawa, H.; Yokozeki, K.; Kumagai, H. Effective Production of 3,4-dihydroxyphenyl-L-alanine (L-DOPA) with Erwinia herbicola cells carrying a mutant transcriptional regulator TyrR. *J. Biotechnol.* **2005**, *115*, 303–306.
[5] Akashi, H.; Gojobori, T. Metabolic Efficiency and Amino Acid Composition in the Proteomes of *Escherichia coli* and Bacillus subtilis. *PNAS.* **2002**, *99*, 3695–3700.
[6] Bongaerts, J.; Kramer, M.; Muller, U.; Raeven, L.; Wubbolts, M. Metabolic Engineering for Microbial Production of Aromatic Amino Acids and Derived Compounds. *Metab. Eng.* **2001**, *3*, 289–300.
[7] Yang, T.; Rao, Z.; Zhang, X.; Xu, M.; Xu, Z.; Yang, S. T. Metabolic Engineering Strategies for Acetoin and 2, 3-Butanediol Production: Advances and Prospects. *Crit. Rev. Biotechnol.* **2017**, *37*, 990–1005.
[8] Ma, Q.; Zhang, Q.; Xu, Q.; Zhang, C.; Li, Y.; Fan, X.; Xie X.; Chen, N. Systems Metabolic Engineering Strategies for the Production of Amino Acids. *Synth. Syst. Biotechnol.* **2017**, *2*, 87–96.
[9] Reznik, E.; Mehta, P.; Segrè, D. Flux Imbalance Analysis and the Sensitivity of Cellular Growth to Changes in Metabolite Pools. *PLoS Comput. Biol.* **2013**, *9*, e1003195.
[10] Phillips, R.; Kondev, J.; Theriot, J.; Garcia, H. *Physical Biology of the Cell*. Garland Science: Abingdon, 2012.
[11] Alon, U. *An Introduction to Systems Biology: design Principles of Biological Circuits*. Chapman and Hall/CRC Press: Boca Raton, 2006.
[12] Tepper, N.; Noor, E.; Amador-Noguez, D.; Haraldsdóttir, H. S.; Milo, R.; Rabinowitz, J.; Liebermeister, W.; Shlomi, T. Steady-State Metabolite Concentrations Reflect a Balance between Maximizing Enzyme Efficiency and Minimizing Total Metabolite Load. *PloS One* **2013**, *8*, e75370.
[13] Muñoz, A.J.; Hernández-Chávez, G.; de Anda, R.; Martínez, A.; Bolívar, F.; Gosset, G. Metabolic Engineering of *Escherichia coli* for Improving L-3, 4-Dihydroxyphenylalanine (L-DOPA) Synthesis from Glucose. *J. Ind. Microbiol. Biotechnol.* **2011**, *38*, 1845.
[14] Wei, T.; Cheng, B.Y.; Liu, J.Z. Genome Engineering *Escherichia coli* for L-DOPA Overproduction from Glucose. *Sci. Rep.* **2016**, *6*, 30080.
[15] Gosset, G. Production of Aromatic Compounds in Bacteria. *Curr. Opin. Biotechnol.* **2009**, *20*, 651–658.
[16] Fernandez-de-Cossio-Diaz, J.; Leon, K.; Mulet, R. Characterizing Steady States of Genome-Scale Metabolic Networks in Continuous Cell Cultures. *PLoS Comput. Biol.* **2017**, *13*, e1005835.
[17] Juminaga, D.; Baidoo, E.E.K.; Redding-Johanson, A.M.; Batth, T.S.; Burd, H.; Mukhopadhyay, A.; Petzold, C.J.; Keasling, J.D. Modular Engineering of L-Tyrosine Production in *Escherichia coli*. *Appl. Environ. Microbiol.* **2012**, *78*, 89–98.
[18] Lutke-Eversloh, T.; Stephanopoulos, G. L-Tyrosine Production by Deregulated Strains of *Escherichia coli*. *Appl. Microbiol. Biotechnol.* **2007**, *75*, 103–110.
[19] Olson, M.M.; Templeton, L.J.; Suh, W.; Youderian, P.; Sariaslani, F.S.; Gatenby, A.A.; Van Dyk, T.K. Production of Tyrosine from Sucrose or Glucose Achieved by Rapid Genetic Changes to Phenylalanine-Producing *Escherichia coli* Strains. *Appl. Microbiol. Biotechnol.* **2007**, *74*, 1031–1040.
[20] Jensen, E.B.; Carlsen, S. Production of Recombinant Human Growth Hormone in *Escherichia coli*: expression of Different Precursors and Physiological Effects of Glucose, Acetate, and Salts. *Biotechnol. Bioeng.* **1990**, *36*, 1–11.
[21] Cabiscol, E.; Tamarit, J.; Ros Salvador, J. Oxidative Stress in Bacteria and Protein Damage by Reactive Oxygen Species. *Int. Microbiol.* **2000**, *3*, 3–8.
[22] Shine, J.; Dalgarno, L. The 3′-Terminal Sequence of *Escherichia coli* 16S Ribosomal RNA: complementarity to Nonsense Triplets and Ribosome Binding Sites. *Proc. Natl. Acad. Sci. U.S.A.* **1974**, *71*, 1342–1346.
[23] Thomason, L.C.; Costantino, N.; Court, D.L. *E. coli* Genome Manipulation by P1 Transduction. *Curr. Protoc. Mol. Biol.* **2007**, 79, 1–17.
[24] Cherepanov, P.P.; Wackernagel, W. Gene Disruption in *Escherichia coli*: Tc R and Km R Cassettes with the Option of Flp-Catalyzed Excision of the Antibiotic-Resistance Determinant. *Gene* **1995**, *158*, 9–14.
[25] Tyagi, N.; Saini, D.; Guleria, R.; Mukherjee, K.J. Designing an *Escherichia coli* Strain for Phenylalanine Overproduction by Metabolic Engineering. *Mol. Biotechnol.* **2017**, *59*, 168–178.
[26] Siddhuraju, P.; Becker, K. Rapid Reversed-Phase High Performance Liquid Chromatographic Method for the Quantification of L-Dopa (L-3, 4-Dihydroxyphenylalanine), Non-Methylated and Methylated Tetrahydroisoquinoline Compounds from Mucuna Beans. *Food Chem.* **2001**, *72*, 389–394.
[27] Bajad, S.U.; Lu, W.; Kimball, E.H.; Yuan, J.; Peterson, C.; Rabinowitz, J.D. Separation and Quantitation of Water Soluble Cellular Metabolites by Hydrophilic Interaction Chromatography-Tandem Mass Spectrometry. *J. Chromatogr. A* **2006**, *1125*, 76–88.
[28] Das, A.; Verma, A.; Mukherjee, K.J. Synthesis of Dopamine in E. coli Using Plasmid-Based Expression System and Its Marked Effect on Host Growth Profiles. *Prep. Biochem. Biotechnol.* **2017**, *47*, 754–760.
[29] Owolabi, J.B.; Rosen, B.P. Differential mRNA Stability Controls Relative Gene Expression within the Plasmid-Encoded Arsenical Resistance Operon. *J. Bacteriol.* **1990**, *172*, 2367–2371.
[30] Newbury, S.F.; Smith, N.H.; Higgins, C.F. Differential mRNA Stability Controls Relative Gene Expression within a Polycistronic Operon. *Cell* **1987**, *51*, 1131–1143.
[31] Coulombel, L.; Nolan, L.C.; Nikodinovic, J.; Doyle, E.M.; O'Connor, K.E. Biotransformation of 4-Halophenols to 4-Halocatechols Using *Escherichia coli* Expressing 4-Hydroxyphenylacetate 3-Hydroxylase. *Appl. Microbiol. Biotechnol.* **2011**, *89*, 1867–1875.
[32] Ballou, D.P.; Entsch, B.; Cole, L.J. Dynamics Involved in Catalysis by Single-Component and Two-Component Flavin-Dependent Aromatic Hydroxylases. *Biochem. Biophys. Res. Commun.* **2005**, *338*, 590–598.
[33] Bren, A.; Park, J.O.; Towbin, B.D.; Dekel, E.; Rabinowitz, J.D.; Alon, U. Glucose Becomes One of the Worst Carbon Sources for E.coli on poor nitrogen sources due to suboptimal levels of cAMP. *Sci. Rep.* **2016**, *6*, 24834
[34] Ginésy, M.; Rusanova-Naydenova, D.; Rova, U. Tuning of the Carbon-to-Nitrogen Ratio for the Production of L-Arginine by *Escherichia coli*. *Fermentation* **2017**, *3*, 60.
[35] El-Mansi, E.M.T.; Bryce, C.F.; Allman, A.R.; Demain, A.L. *Fermentation Microbiology and Biotechnology*. CRC Press: Boca Raton, 2011.
[36] Bennett, B.D.; Kimball, E.H.; Gao, M.; Osterhout, R.; Van Dien, S.J.; Rabinowitz, J.D. Absolute Metabolite Concentrations and Implied Enzyme Active Site Occupancy in *Escherichia coli*. *Nat. Chem. Biol.* **2009**, *5*, 593.
[37] List of important data bases used 1. Brenda: https://www.brenda-enzymes.org/ For enzyme-related quarries. 2. KEGG: http://www.genome.jp/kegg/pathway.html For sequence-related quarries. 3. EcoCyc: https://ecocyc.org/ For pathway-related quarries. 4. NCBI: https://www.ncbi.nlm.nih.gov/ For BLAST algorithm tools. 5. NEB Cutter: http://nc2.neb.com/NEBcutter2/ For restriction digestion-related queries.
[38] List of resource repositories used 1. ADDGENE: https://www.addgene.org/ Ordering plasmid constructs. 2. CGSC: http://cgsc2.biology.yale.edu/ Ordering mutants for transferring deletions. 3. ATCC: https://www.atcc.org/Products/All/25404.aspx Ordering K-12 wild type, nonlysogenic P1 phage for transducing *Escherichia coli* K12.
[39] Mass spectra library consulted: https://chemdata.nist.gov/For compound identification from mass-spec peaks.